

DOI: 10.24425/amm.2019.130100

M. MIKUŚKIEWICZ*[#], G. MOSKAL***SOLID STATE SYNTHESIS OF EUROPIUM ZIRCONATE BASED MATERIAL**

In the article, the characterization of the microstructure, phase composition and distribution of elements in the $\text{Eu}_2\text{O}_3\text{-ZrO}_2$ sintered materials obtained by four different ways of powders' homogenization (mixing) process and different temperature of sintering process is shown. The feedstock powders with an average mole ratio of ZrO_2 to Eu_2O_3 equal 74% to 26% were used as an initial material. The principal aim of the investigation was characterization of differences in the microstructure of the same type of ceramics, however, prepared via different mixing and manufacturing processes. The range of the investigation covered a characterization of these materials via phase identification of all samples by XRD (*X-ray diffraction*) and characterization of internal morphology of the specimens with detailed analysis of elements distributions by SEM (*scanning electron microscopy*) and EDS (*energy dispersive spectrometry*). The aim of the following investigation is to characterize the possibilities of the solid state synthesis of the europium zirconate based materials, dedicated for TBC applications.

Keywords: europium zirconates, solid-state synthesis, pyrochlores, TBC

1. Introduction

Gas turbines installed in aircraft engines work in one of the most aggressive environments. These elements are exposed to high mechanical stresses and high temperatures, moreover the discussed components are exposed to the impact of erosion and corrosive media. This fact drives the continuous need to modernize and improve the materials and technological solutions in the elements used in such challenging machine that is aircraft engine [1-3]. In recent years, widely promoted solution is the development of new thermal barrier coatings (TBC) based on ceramic materials characterized by the structure of a pyrochlore. The pyrochlore unit cell can be perceived as eight elementary cells of fluorite, each of which comprises, on average, a single oxygen vacancy. The stoichiometric general formula of pyrochlore structure is $\text{A}_2\text{B}_2\text{B}'_2\text{O}_7$, where A – are usually rare earth metals, whereas B are transition metals. The most promising materials in this group proved to be zirconates of La, Gd, Nd, Sm and Eu. Compounds with the pyrochlore structure $\text{RE}_2\text{Zr}_2\text{O}_7$ are characterized by many desirable properties, among others: very low thermal conductivity coefficient – below 2.0 W/mK; high coefficient of thermal expansion – over $10^{-5} \text{ }^\circ\text{C}^{-1}$; operating at temperatures up to 1600°C [4-12].

2. Research methodology

In the investigation, the following input materials were used: nanocrystalline powders of zirconium oxide ZrO_2 , provided by (Hefei EvNano Technology Co., Ltd., total contaminants less than 0.5 wt%) and europium oxide Eu_2O_3 (Inframat Advanced Materials, LLC, purity 99,995% (REO)). For zirconia particles, the size of conglomerates was ca. 150 nm, whereas the size of elementary particles was in the range of 60÷120 nm. For europium oxide particles, the size of conglomerates was higher than 200 nm of the grain radius, whereas the size of the smallest elementary particles was lower than that for zirconia. The size of the discussed small elementary particles was at level of 30÷80 nm [13]. On the basis of the X-ray diffraction analysis of the tested powder, the phase identification concerning the starting powder was performed. XRD measurements were performed in the 10-90° 2θ range with Cu K_α radiation equipped with an incident beam monochromator (X'pert, Philips-Panalytical). Afterwards, these powders undergone further metallographic evaluation.

The powders were weighed in the weight ratio of 1:1 that gives the mole ratio of ZrO_2 to Eu_2O_3 as 74% to 26%. Taking into account the mole ratio, occurred an excess of zirconium oxide as to the stoichiometric pyrochlore structure. In the case of pyrochlore-structured compounds, the mole ratio is 67% to 33%. The aim was to get acquainted with the mechanism of synthesis and identification of intermediate phases.

* SILESIAAN UNIVERSITY OF TECHNOLOGY, INSTITUTE OF MATERIALS ENGINEERING, 8 KRASIŃSKIEGO STR., 40-019 KATOWICE, POLAND

Corresponding author: marta.mikusiewicz@polsl.pl

In the next part, the powders were subjected to the process of mixing and homogenization, which was carried out by four methods, indicated in the order DM, MA, USA, MUA:

- DM – the composition was prepared by mixing the components in the agate mortar for 15 min,
- MA – the composition was prepared by the wet mechanical mixing the components with ethanol in an agate mortar for 15 min,
- USA – the composition was prepared by mixing of the components in ethanol with the ultrasound – assisted mixing for 3 hours,
- MUA – the composition was prepared by mechanical mixing of the components in ethanol with the additional ultrasound-assisted mixing in alcohol-ethanol for 3 hours.

The next step was to prepare a sinter. This task was carried out by two methods, labeled in sequence as high temperature sintering under pressure (HTSP) and high temperature sintering under pressure with additional annealing (HTSPA). The selection of sintering method has a significant impact on the synthesis process of the final europium zirconate based materials. This impact is related with the phase composition, degree of homogeneity and superstructure creation related with ordering/disordering phenomena. The application of sintering process with high temperature vacuum press allows to obtain the final material with the best homogeneity from phase composition point of view, as described in the article [13].

The HTSP process was realized in high temperature vacuum press by Degussa. The sintering temperature was 1350°C (with a heating rate of approximately 30°C/min and a free cooling with a furnace) with the time of process equal 2 h. The compaction pressure was 15 MPa, whereas the whole sintering process was made in a vacuum on the level of 10^{-2} Tr. The HTSPA process was similar to that of described earlier, whereas, additional heat treatment at 1450°C for 5h was performed.

The obtained final materials were analyzed for in view of their phase composition and internal morphology by X-ray diffraction method and scanning electron microscopy (SEM, Hitachi S-3400N) with energy dispersion spectrometry (EDS, Thermo Noran System Seven – measurements were performed with 25 keV, live time 100 s, time constant – automatically, dead

time 30%-40% time of analysis, take-off angle 35°, working distance 10 mm. Moreover, additional optical microscopy (OM) observations were performed.

3. Results

The XRD patterns of the feedstock powders used to the synthesis of final material are shown in Fig. 1. The powder of ZrO_2 type was characterized by occurrence monophasic phase composition; the only one detected phase was zirconia of monoclinic type. Any other types of this oxide were not detected. Fig. 1 shows the experimental XRD pattern of Eu_2O_3 powder. The main detected phase was europia with cubic crystal system, moreover, a small addition of monoclinic crystal phase with the same chemical composition was observed.

The utilized powder is built from conglomerates of nanosized, inter connected spherical particles. However, these particles do not form any greater structure. In the case of Eu_2O_3 powder morphology, the polyhedral particles are dominant. In some cases, the surfaces of discussed particles are built from conglomerates of nanosized spherical particles, similarly to the case of ZrO_2 .

The another step of investigation concerned the synthesis of europium zirconates using different methods of feedstock powder mixing and various sintering parameters. The obtained materials were characterized from the morphological homogeneity point of view. Visual studies did not show substantial differences, however, in the case of material mixed by DM method, the visual inspection revealed differences in internal morphology of sintered material in comparison to that of sinters obtained by other methods of mixing. The method of the feedstock powders homogenization significantly affects the phase uniformity of the final sintered materials. This effect is noticeably visible, especially in the case of alcohol-free method of mixing such as DM, where the inhomogeneity of structural elements was very high. For those cases, where the alcohol was used, the homogeneity level was much higher, especially in the case of mechanical mixing MA. The application of ultrasound (USA, MUA) did not provide any additional beneficial effect

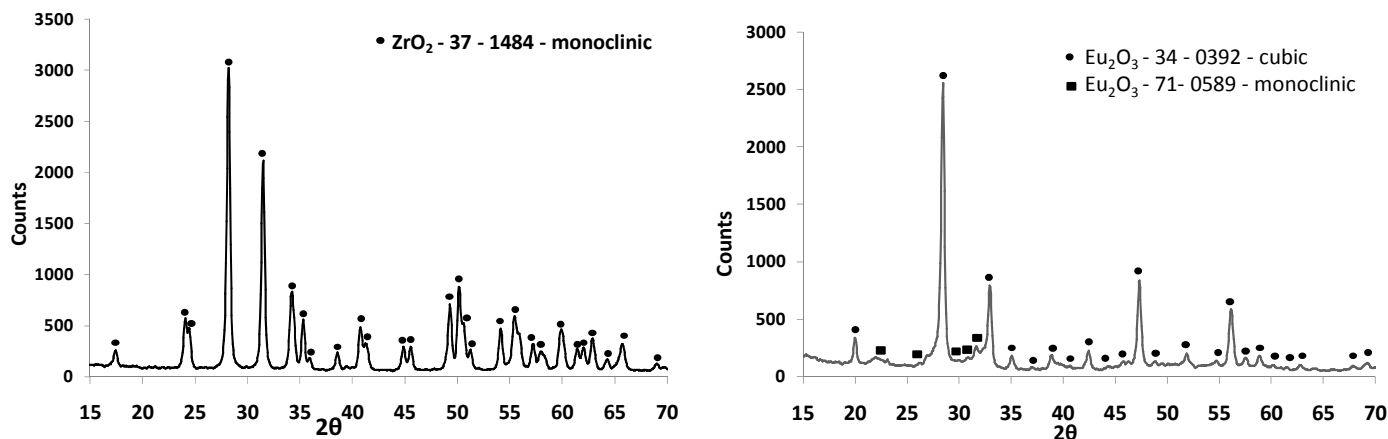


Fig. 1. XRD pattern of ZrO_2 oxide and Eu_2O_3 oxide used to synthesis of Eu zirconates

in comparison to the MA method. The SEM and EDS analysis showed a strong segregation in the case of sinter which was homogenized by DM method (Fig. 2). Not reacted areas of zirconia were observed in principle (point 3) in the form of polyhedral grains (or rather initial sintered ZrO_2 powder granules) as well as a diffusion areas in the form of massive layer (point 2) covering zirconia areas. The lighter structural elements in the analyzed sinter are areas with similar content of Eu and Zr. Relative standard deviations of concentrations (δ_c) were 2.7 wt% for Zr and 0.05 wt% for Eu.

In the case of material after the MA process, the dominant observable areas were the zones with similar content of Zr and Eu (ratio 57 to 43 – almost identical like in the case of DM

specimen). Additionally, areas with lower content of Eu were observed. In the case of these areas, content of europium was ca. 10 wt% lower. There are massive areas without presence of granules-like morphological forms similar to that of initial powders. The morphology of the discussed zone implies that a synthesis of new phase took place. In such areas, the content of Eu_2O_3 should be lower in comparison to that of lighter areas. Similar effect were observed in the case of USA and MUA specimens (Fig. 3), however, the size of those zones was much higher or substantially lower Eu_2O_3 content was detected (only in USA specimen).

A relatively high correlation between the microstructure investigation and XRD phase analysis was revealed in the case

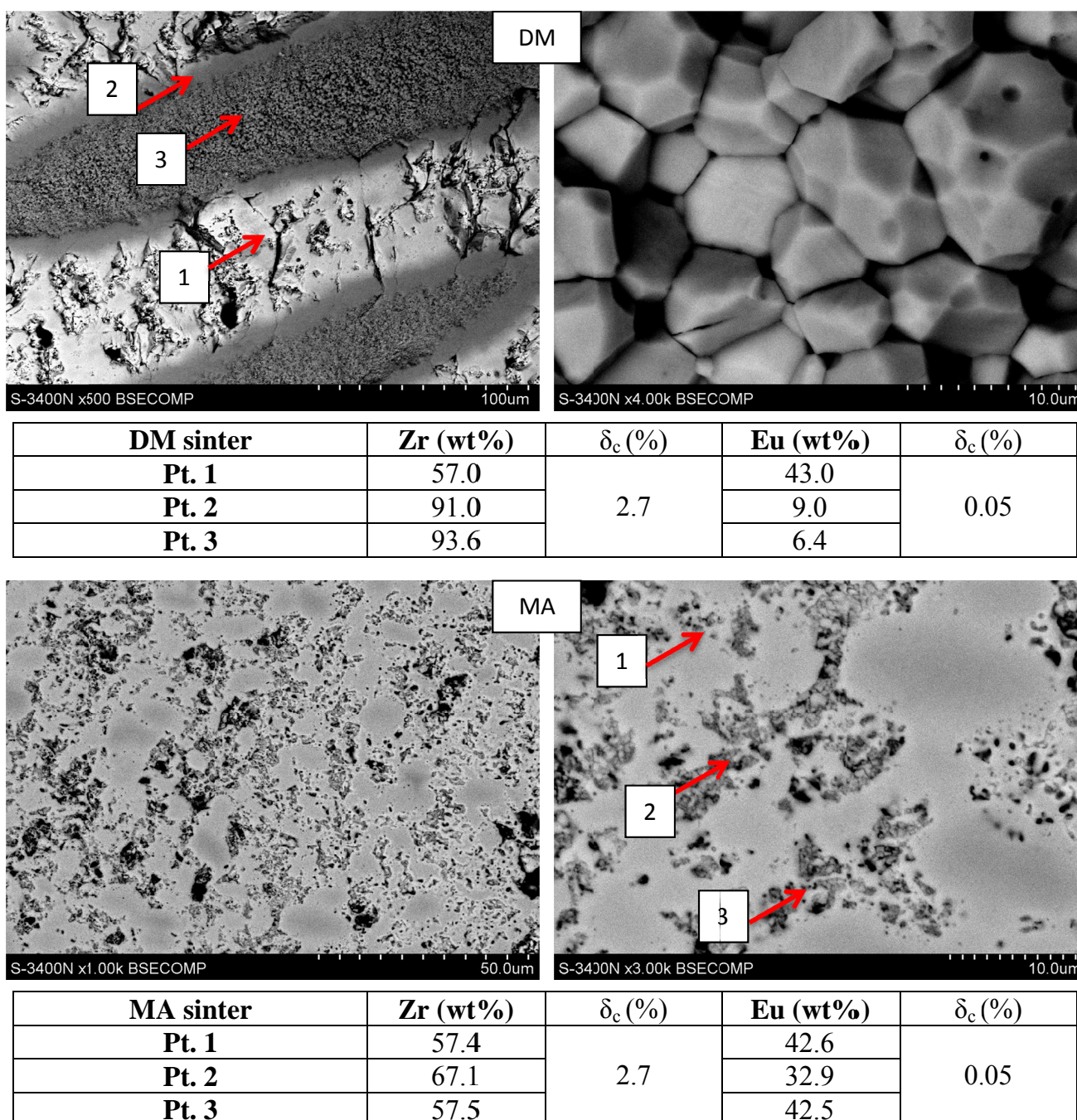


Fig. 2. Morphology of sintered materials of ZrO_2 - Eu_2O_3 type after DM and MA processes

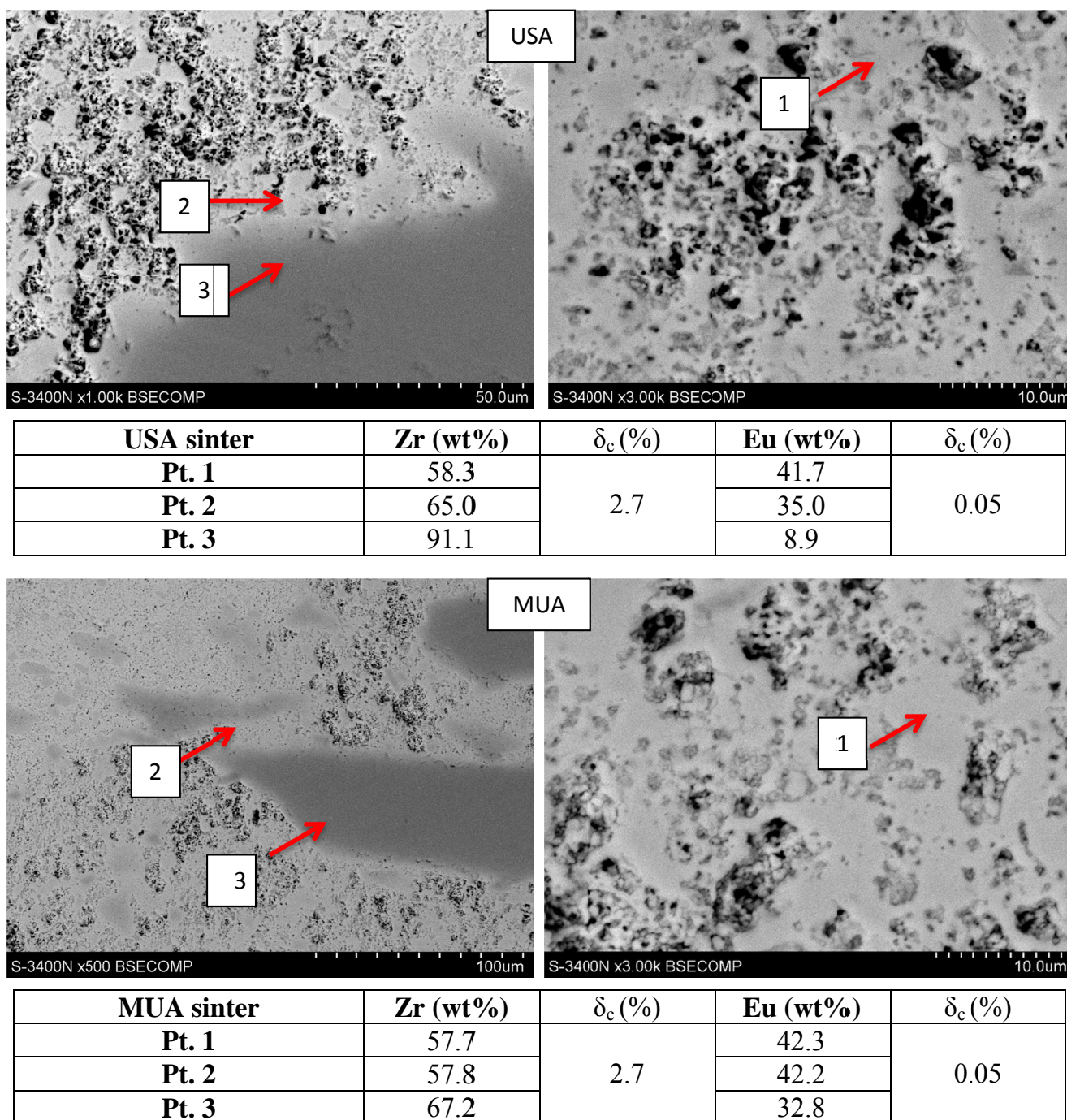


Fig. 3. Morphology of sintered materials of ZrO_2 - Eu_2O_3 type after USA and MUA processes

of the analyzed materials, especially taking into account the inhomogeneity. In the experimental XRD pattern of DM material – HTSP (Fig. 4a), reflexes corresponding to different types of zirconates may be distinguished. The $Eu_2Zr_2O_7$ with pyrochlore (P) type of lattice was detected as a dominant phase. Moreover, the detailed analysis of XRD line profile implies a presence of other zirconates phases of $Eu_{0.5}Zr_{0.5}O_{1.75}$ type and nonstoichiometric $Eu_{0.2}Zr_{0.8}O_{1.9}$. However, the previously mentioned additionally detected phases were characterized by fluorite (F) type of lattice. The detected dominant pyrochlore phase was characterized by presence of a superstructure which. The occurrence of such phase suggests a strong effect of lattice ordering (peaks marked

by yellow color – 2θ angles: 14.56; 28.13; 37.28; 44.69; 51.28; 52.07; 57.36). The zirconate of europium $Eu_{0.5}Zr_{0.5}O_{1.75}$ with the fluorite structure has a formula identical in comparison to that of pyrochlore phase, however, the f-type zirconate does not show the ordering effect and is characterized by different lattice parameters. Additionally, the diffraction peaks corresponding to oxide identified as an isomorphous phase $(Eu, Lu_{0.5}Ta_{0.5})O_3$ were revealed – this phase is an impurity most likely from the test chamber. It should be oxide of $(Eu, Zr)_2O_3$ type with cubic structure (C type), generated as an effect of inter-solution process of initial oxides. The last identified phase was monoclinic zirconia, which was added with an excess to the powder mixture.

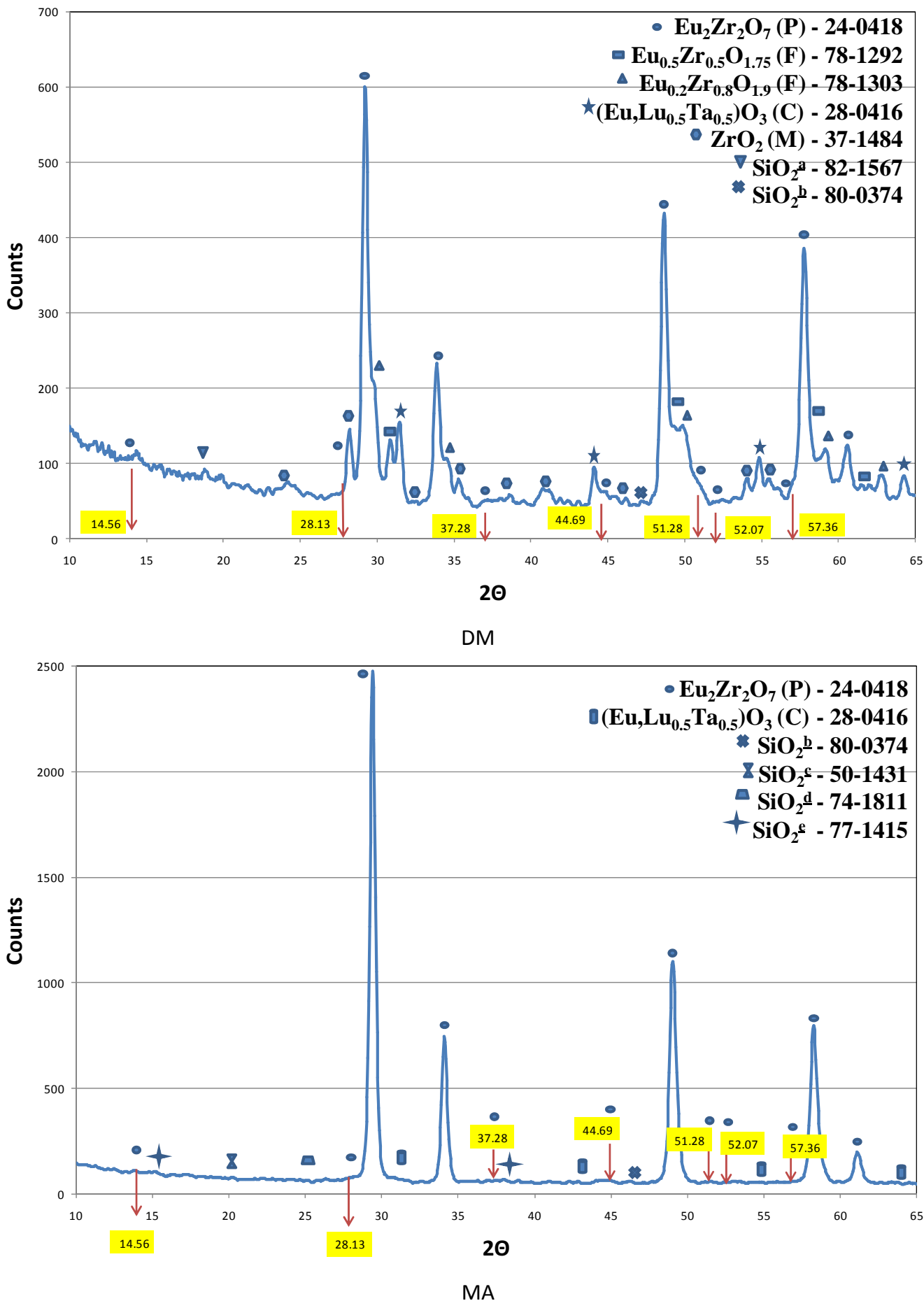


Fig. 4a. XRD diffraction patterns of sintered materials of $\text{ZrO}_2\text{-Eu}_2\text{O}_3$ type after DM and MA processes (HTPS)

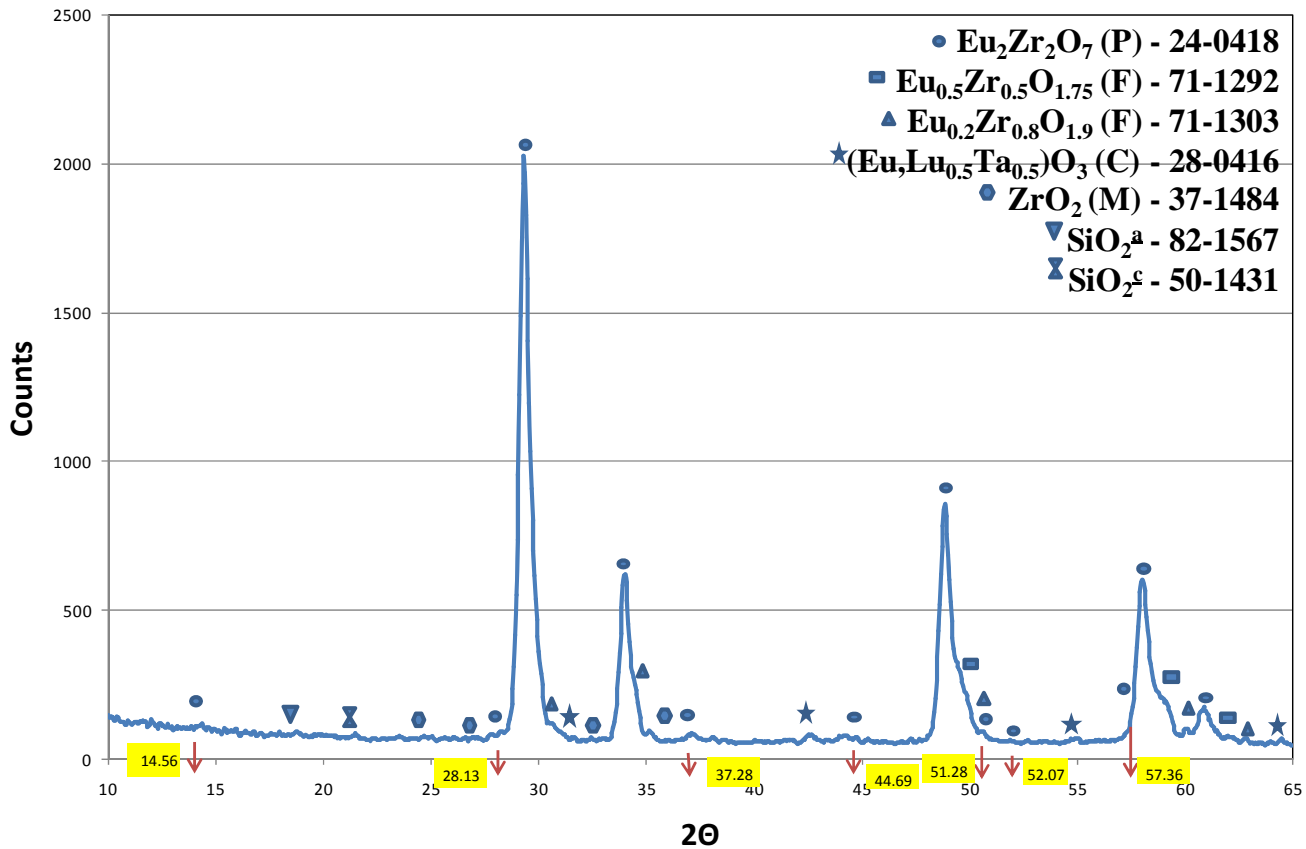
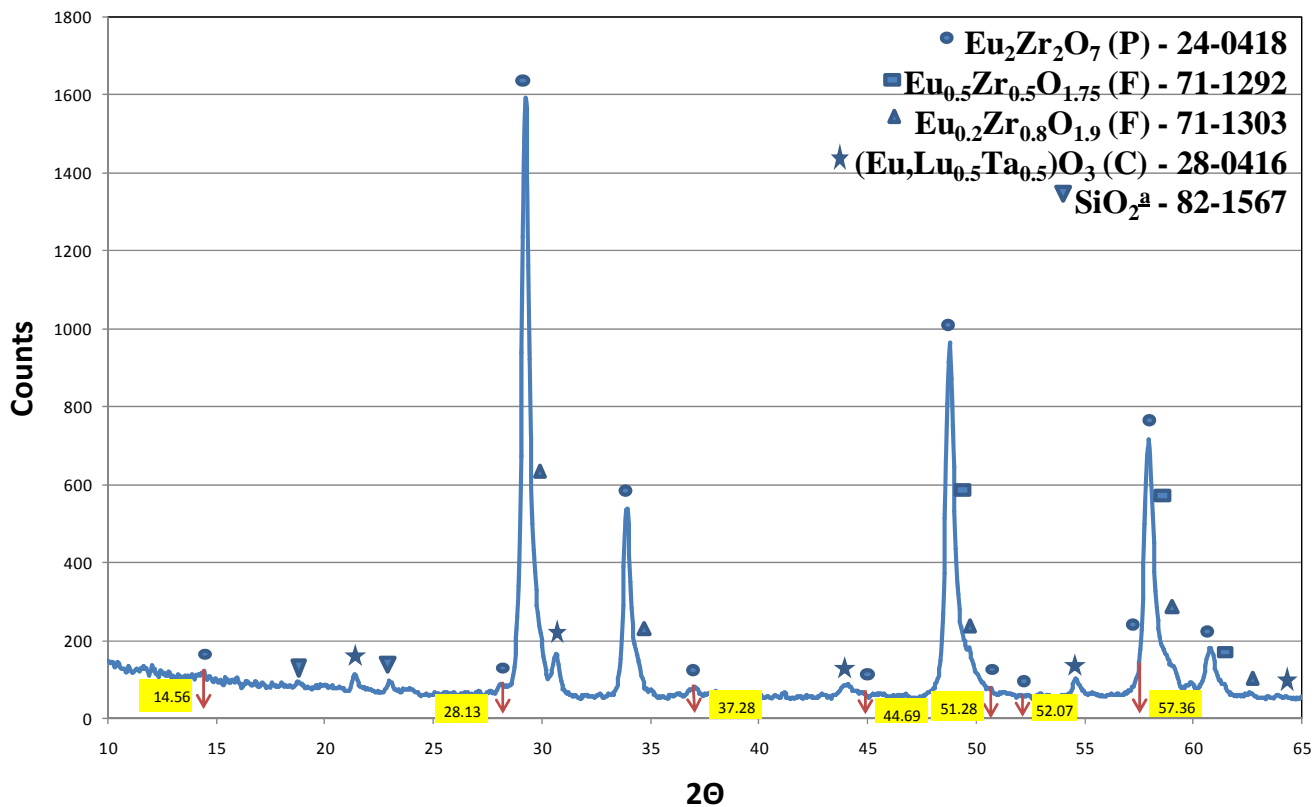


Fig. 4b. XRD diffraction patterns of sintered materials of $\text{ZrO}_2\text{-Eu}_2\text{O}_3$ type after USA and MUA processes (HTPS)

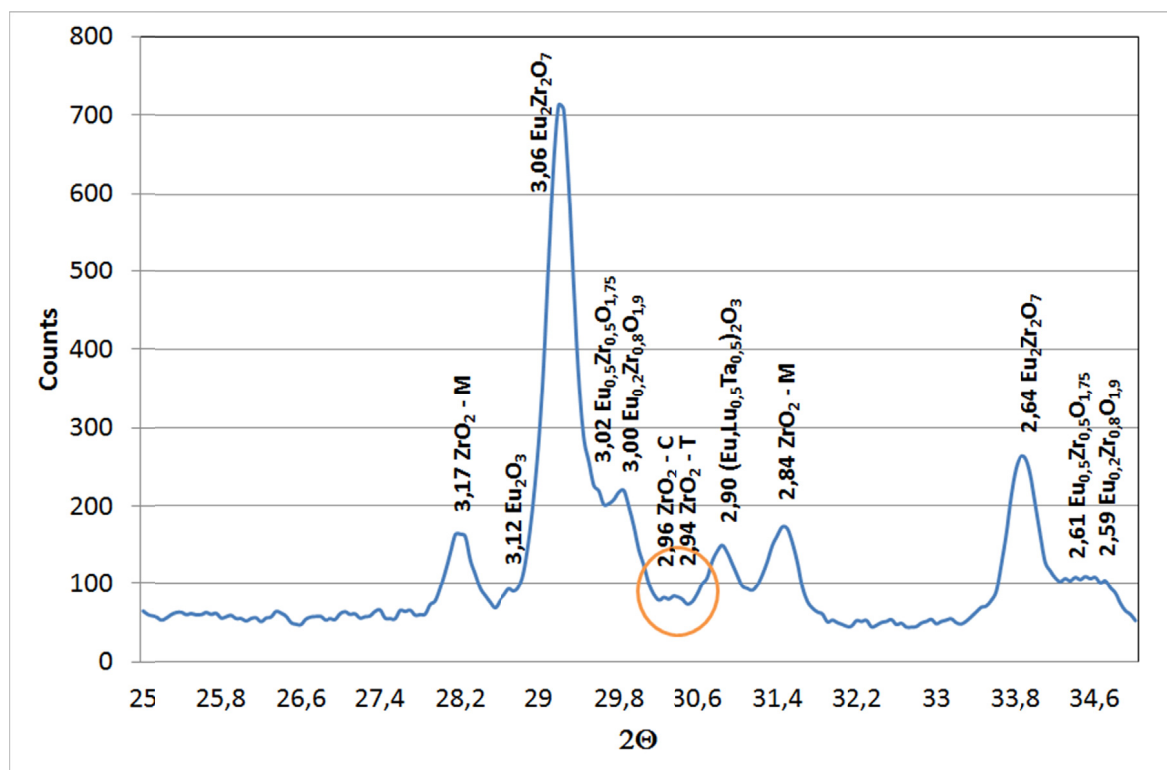


Fig. 5. XRD diffraction pattern of DM sintered materials of ZrO_2 - Eu_2O_3 type (HTPS)

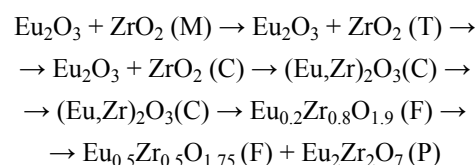
The analysis of the diffraction pattern in a very narrow range showed that probably, the tetragonal and cubic zirconia are present as well – HTSP (Fig. 5). The low-intensity SiO_2 reflections are connected with a presence of some impurities in the starting powders. In the case of MA sinter, the peaks corresponding to the identified phases other than the pyrochlore were characterized by much lower intensity. For this material the phase structure was almost monophasic; the dominant $Eu_2Zr_2O_7$ desirable phase was detected. Although a presence of $(Eu,Zr)_2O_3$ oxide was possible, the peaks corresponding to this phase were very weak. The reflexes connected with the pyrochlore phase were very smooth, without any shift from the right position. The XRD pattern implies a lack of other types of zirconate phases such as in the case of DM material. The similar condition was noticed in the case of a diffraction pattern obtained for USA process. For this material, an effect of right-site extending was observed and probably the fluorite types of zirconates were present in this case. Very weak peaks corresponding to $(Eu,Zr)_2O_3$ and monoclinic ZrO_2 were detected as well. The last analyzed diffraction pattern (MUA material) was the most similar to DM material and revealed a presence of peaks related with $(Eu,Zr)_2O_3$ phase and fluorite types of zirconates.

Other interesting information revealed during the X-ray diffraction analysis was an effect of superstructure. The diffraction peaks related with the superstructure are characterized by higher intensity in sinters with heterogeneous and more complexed structure in comparison to that of the case of DM – HTSP (Fig. 4a), USA and MUA materials – HTSP (Fig. 4b). This state of affairs is caused by an influence of ZrO_2 on organization of the pyrochlore structure [14-15]. In the analyzed cases, the high

level of inhomogeneity is related with a lower value of zirconia in the pyrochlore phase. As a consequence, a higher level of peaks intensity related with pyrochlore superstructure was observed. On the other hand, the pyrochlore crystal system characterized by high degree of structure order has ability to dissolve in ZrO_2 in some extent. In the case of MA material with about 7% molar excess of ZrO_2 and the highest level of homogeneity (related with presents only pyrochlore phases reach in zirconia), the intensity of superlattice peaks were the smallest.

The phase analysis after 5 hours of heating at temperature $1450^\circ C$ – HTSPA is shown in Fig. 6a and 6b, where the most intensive changes may be observed in the case of specimen marked as DM.

The observed changes included a creation of zirconate phase with higher level of dissolved zirconia and a disappearance of $(Eu,Zr)_2O_3$ oxide (revealed as isomorphic $(Eu,Lu_{0.5}Ta_{0.5})O_3$ phase). This effect was observed especially in the case of DM material. In general, the observed sequence of phase creation can be expressed as follow:



From morphological point of view, the observed changes are related only with formation of zirconate phases with higher concentration of zirconia, whereas the microstructure of materials after HTSPA process were very similar to that of observed for initial sintered pellets in Fig. 2 and in Fig. 3.

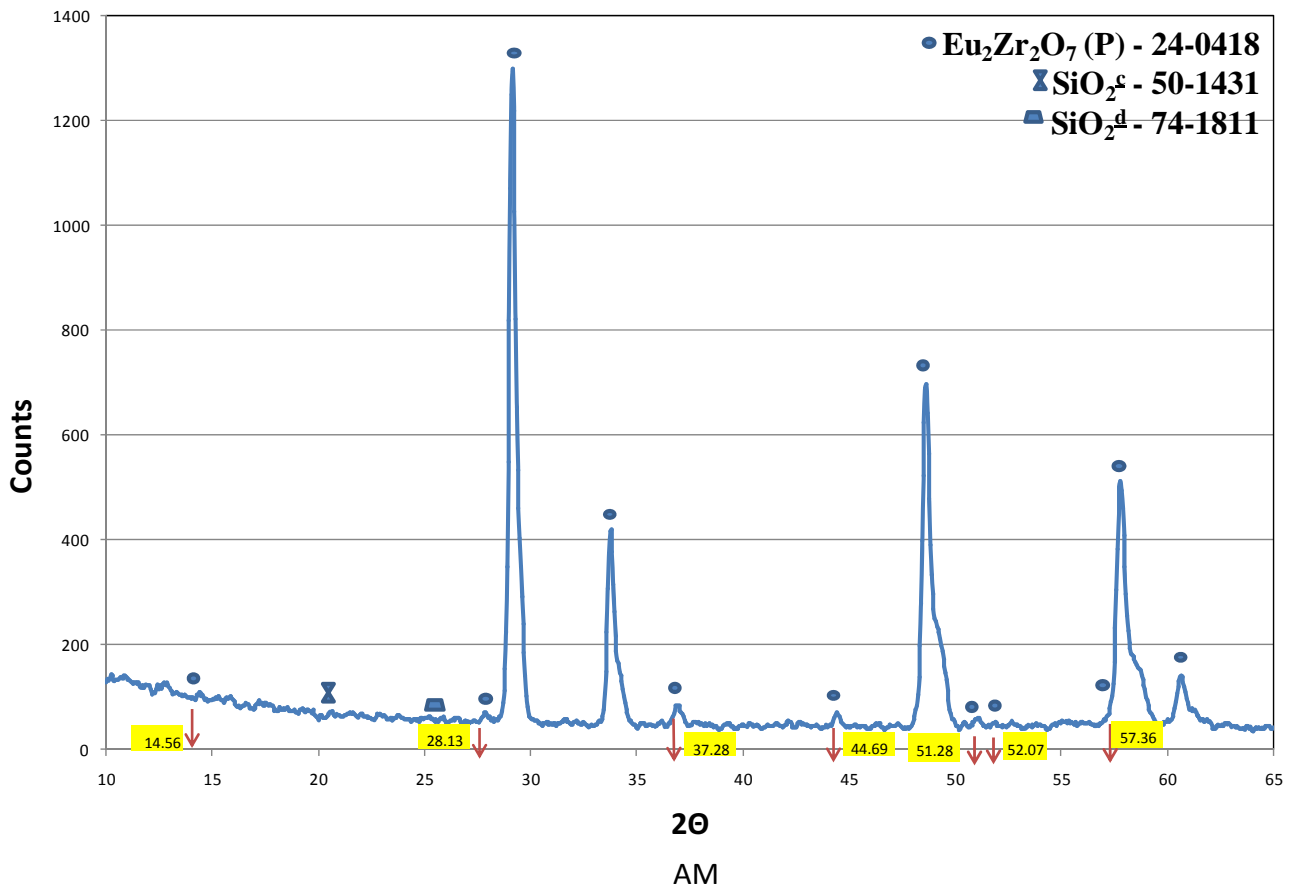
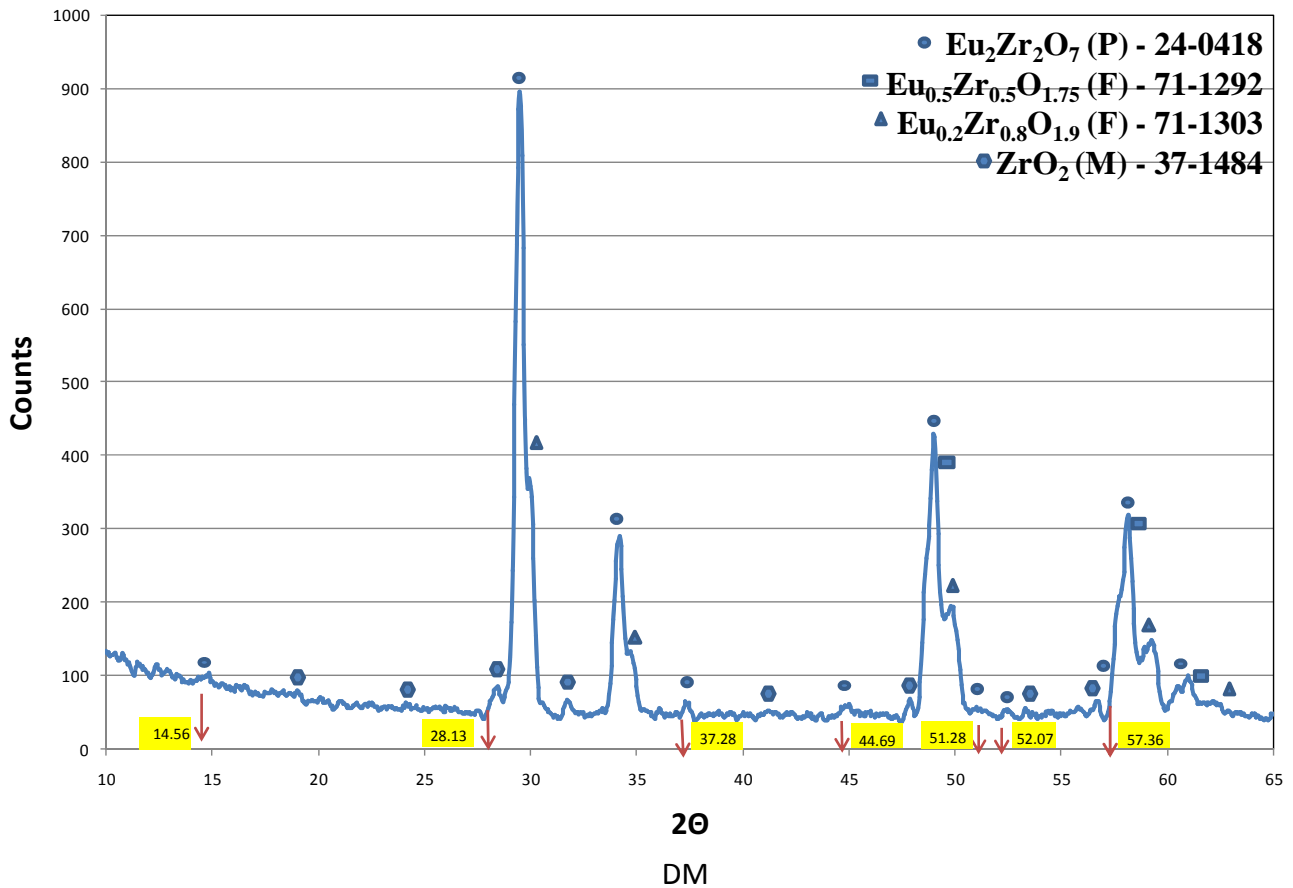


Fig. 6a. XRD diffraction patterns of sintered materials of $\text{ZrO}_2\text{-Eu}_2\text{O}_3$ type after annealing process at temperature 1450°C after DM and MA processes (HTPSA)

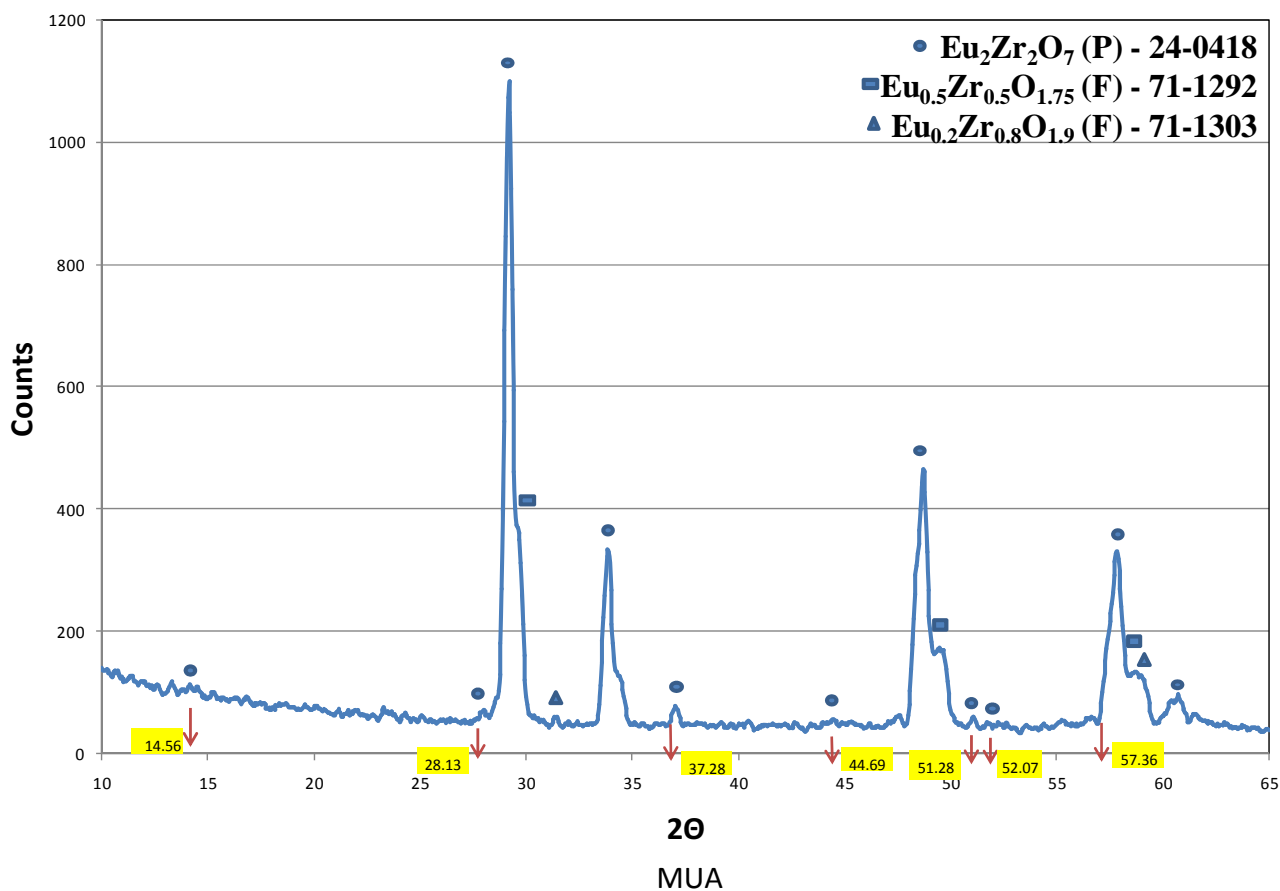
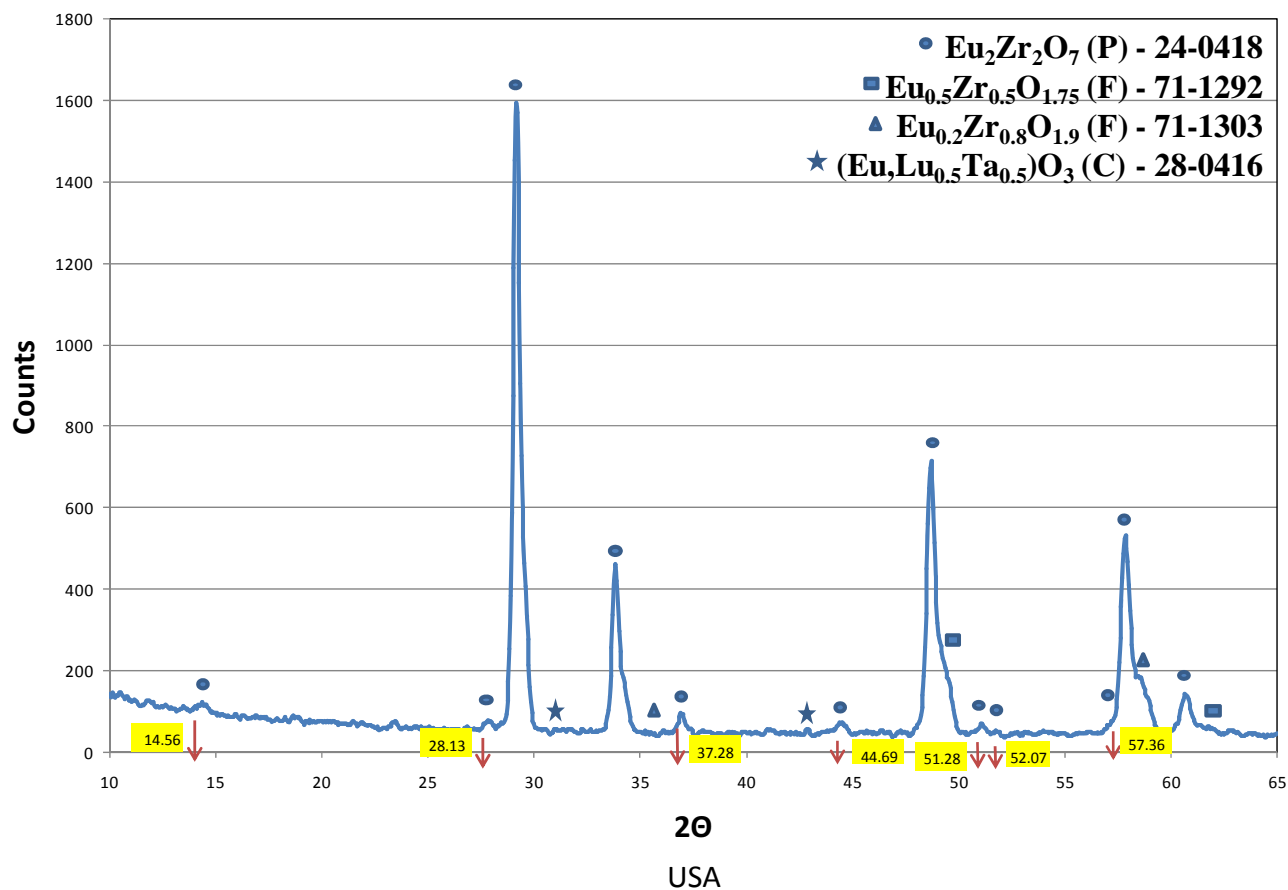


Fig. 6b. XRD diffraction patterns of sintered materials of $\text{ZrO}_2\text{-Eu}_2\text{O}_3$ type after annealing process at temperature 1450°C after USA and MUA processes (HTPSA)

4. Summary

The solid state synthesis of europium zirconate strongly depend on the method of powder preparation. The most uniform final material was obtained in the case of mechanical mixing in alcohol. In other cases the morphology of sinters was substantially inhomogeneous and porous, typical for solid state synthesis of ceramic materials [16].

Ultrasound-assisted mixing method did not provide satisfactory results. The quality of obtained sinters was much higher than that of ceramics synthesized from dry mixed powder, however, the material was still characterized by considerable inhomogeneity.

The application solid state synthesis of wet mechanically mixed powders with subsequent synthesis in high-temperature vacuum press and continuous pressing in vacuum provided the possibility to obtain the relatively uniform final material based of europium zirconate. On the other hand, the other methods of initial powder mixture preparation made the possibility to observe transition stages of sintering process and characterize the formation of different complex oxides. In this case, the synthesis from ZrO_2 and Eu_2O_3 powders to the final stoichiometric $Eu_2Zr_2O_7$ with pyrochlore type of lattice was described.

Applied of additional annealing of sinters at temperature $1450^\circ C$ changed the phase composition only in the very narrow range and practically did not change the internal morphology of the sinter. The phase changes were related with the formation of zirconates phase with higher concentration of zirconia.

On the other hand, the obtained inhomogeneous morphology of sinters gave possibility of observation of phase creation sequence, especially formation of nonstoichiometric zirconates of europium. This effect was enhanced by slight excess of zirconia in relation to europium oxide in the mixture of input powders.

Acknowledgments

This work was supported by the National Science Centre, Poland under grant number 2016/21/D/ST8/01687.

REFERENCES

- [1] F.C. Toriz, A.B. Thakker, S.K. Gupta, ASME-88-GT-279, 1 (1988).
- [2] K.D. Sheffler, D.K. Gupta, ASME-88-GT-286, 1 (1988).
- [3] S.M. Meier, D.M. Nissley, K.D. Sheffler, T.A. Cruse, J. Eng. Gas Turb. Power **114**, 258-263(1992).
- [4] M.J. Malony: U.S. Patent 6,284,323 (2001).
- [5] R. Subramanian: U.S. Patent 6,387,539 (2002).
- [6] I. Bauer, Tribologia 1, 17-21 (2017).
- [7] R. Vaben, F. Traeger, D. Stover: Int. J. Appl. Ceram. Technol. **1**, 356 (2004).
- [8] M. Mikuškievicz, G. Moskal, D. Migas, M. Stopyra, Ceram. Int. **42** (2 B), 2760-2770 (2019).
- [9] G. Moskal, M. Mikuškievicz, DefectDiffus Forum **336**, 91-96 (2013).
- [10] S.V. Ushakov, A. Navrotsky, J. Am. Ceram. Soc. **90**, 1171-1176 (2007).
- [11] X. Cao, Z. Ma, Y. Liu, Z. Du, K. Zheng, Rare Metal Mat. Eng. **42**, 1134-1138 (2013).
- [12] Q. Shen, L. Yang, Y.C. Zhou, Y.G. Wei, N.G. Wang, Surf. Coat. Technol. **325**, 219-228 (2017).
- [13] S. Jucha, G. Moskal, M. Mikuškievicz, M. Stopyra, Acta Phys. Pol. A **130**, 866-868 (2015).
- [14] O. Fabrichnaya, M.J. Kriegel, D. Pavlyuchkov, J. Seidel, A. Dzuban, G. Savinykh, G. Schreiber, Thermochem. Acta **558**, 74 (2013).
- [15] A.V. Shlyakhtina, A.V. Knotko, M. Boguslavskii, S.Y. Stefanovich, I.V. Kolbanev, L.L. Larina, L.G. Shcherbakova, Solid State Ion. **178**, 59 (2007).
- [16] M. Mikuškievicz, M. Stopyra, G. Moskal, Solid State Phenom **223**, 54 (2015).